ROCK PHYSICS DIAGNOSTICS OF NORTH SEA SANDS: LINK BETWEEN MICROSTRUCTURE AND SEISMIC PROPERTIES

PER AVSETH, JACK DVORKIN, AND GARY MAVKO
Department of Geophysics, Stanford University, CA 94305-2215, USA

JOHANNES RYKKJE
Norsk Hydro Research Center, 5000 Sandsli, Bergen, Norway

December 2, 1999

ABSTRACT

Velocity in high porosity sands strongly depends on the position and amount of intergranular material. This material may be diagenetic cement that envelops the grains and cements their contacts, small particles that fill the pore space between the larger grains, or a combination thereof. Velocity is high if the original grains are cemented at their contacts. It is low if the pore-filling material is placed away from the contacts. The amount of contact cement and non-cement pore-filling material can be theoretically determined from velocity and porosity using mathematical rock physics diagnostic. Such diagnostic is conducted by adjusting an effective-medium theoretical model curve to a trend in the data and then assuming that the microstructure of the sediment is such as used in the model. We apply this method to log data from two wells that penetrate the North Sea Heimdal formation comprised of Paleocene turbidite sands. The result shows that the pay-zone sand in one well has slight contact cementation, while it is completely uncemented and friable in the other well. This conclusion is directly supported by a cathode-luminescent thin section image. It is also consistent with the depositional environment in the wells. Sands in both wells are very clean. Contact cementation is possible in the first well because the well-sorted large quartz grains do not have any clay or organic coating. On the contrary, contact cementation is absent in the second well, which can be explained by the fact that there quartz grains are covered with small amounts of organic material that prevents contact cement generation. The rock physics diagnostic used here is important for establishing a velocity-porosity trend consistent with local geology. Such trends, used together with seismic inversion data can improve the accuracy of porosity prediction from seismic.

INTRODUCTION

Relations between the elastic rock properties and porosity are needed to infer porosity from seismic data. Velocity-porosity relations may be complicated because the stiffness of rock depends not only on porosity and mineralogy but also on the rock's microstructure (texture), i.e., the arrangement of the components of the solid phase at the pore scale. To appreciate the influence of microstructure, consider Figure 1 where the P-wave velocity is plotted versus porosity for sands. Although, all samples from Figure 1 have high quartz content, the velocity may span as much as 2 km/s in the same porosity range.

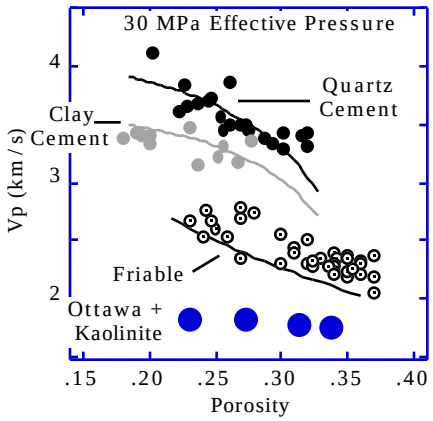

Figure 1. The elastic-wave velocity versus porosity for quartz- and clay-cemented fast North Sea sands; friable North Sea sands (the North Sea data and the models discussed in Dvorkin and Nur, 1996); and hand-made Ottawa sand and kaolinite mixture (data from Yin, 1993). All data are for room-dry samples at 30 MPa differential pressure.

By superimposing theoretical model curves on this cross-plot, we can sort (***diagnose***) the data into the following groups: (a) North Sea sands with small amounts of quartz cement at grain contacts; (b) sands from the same formation but with clay cement; and (c) North Sea friable sands. The slowest group in Figure 1 are hand-made mixtures of Ottawa sand and kaolinite (Yin, 1993), with pure sand at the highest porosity and sand with 15% clay by weight at the lowest porosity. The texture of these mixtures is such that kaolinite fills the pore space between the quartz grains without affecting velocity.

The ***rock physics diagnostic*** illustrated in Figure 1 often provides practically-important information about rock properties. For example, Dvorkin and Brevik (1999) use this method to assess rock strength and permeability in a North Sea well.

In this paper we apply rock physics diagnostic to well log data from two wells drilled through the sands of the Heimdal formation in the North Sea. The oil-saturated pay-zone sands produce distinctive (and separate for each well) velocity-porosity trends. These trends are parallel to each other in the velocity-porosity plane with the velocity difference about 500 m/s.

Rock physics diagnostic implies that this velocity difference is due to small amounts of contact quartz cement present in one well and complete absence of such cement in the other well. A thin-section cathode-luminescent image confirms our mathematical diagnostic.

Texture identification appears to be crucial in the sands under examination because the pay zone can produce drastically different seismic response depending on whether the sand is truly unconsolidated (friable) or has initial quartz cementation. Also, textural changes, if not properly identified, may be misinterpreted in seismic data as pore-fluid changes leading to serious reservoir characterization errors.

THEORETICAL MODELS FOR ROCK DIAGNOSTIC

Dvorkin and Nur (1996) introduced two theoretical models for high-porosity sands (see model curves in Figure 1). The ***contact-cement model*** assumes that porosity reduces from the initial porosity of a sand pack due to the uniform deposition of cement layers on the surface of the grains. This cement may be diagenetic quartz, calcite, or authigenic clay (such as illite). The contact cement dramatically increases the stiffness of the sand by reinforcing the grain contacts.

The ***friable-sand model*** assumes that porosity reduces from the initial sand-pack value due to the deposition of the solid matter away from the grain contacts. Such process of porosity reduction may correspond to deteriorating grain sorting. This non-contact additional solid matter weakly affects the stiffness of the rock.

We introduce another, ***constant-cement***, model which assumes that sands of varying porosity all have the same amount of contact cement. Porosity variation is solely due to non-contact pore-filling material (e.g., deteriorating sorting).

Mathematically, this model is a combination of the contact-cement model, where porosity reduces from the initial sand pack porosity to porosity φ_b due to contact

cement deposition, and the friable-sand model where porosity reduces from φ_b due to the deposition of the solid phase away from the grain contacts (Figure 2).

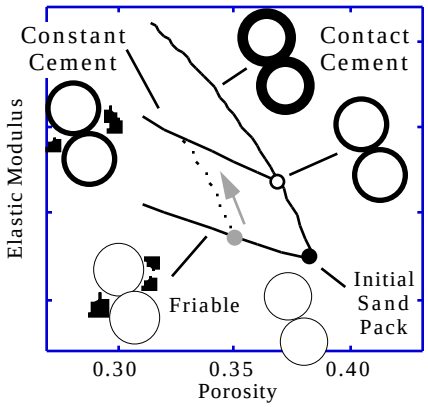

Figure 2. Schematic depiction of three effective-medium models for high-porosity sands in the elastic-modulus-porosity plane and corresponding diagenetic transformations. The elastic modulus may me compressional, bulk, or shear.

To use the constant cement model, one has first to adjust the initial-cement porosity φ_b that corresponds to the point shown as an open circle in Figure 2. The dry-rock bulk and shear moduli at this porosity (K_b and G_b, respectively) are calculated from the contact-cement model (see equations in Dvorkin and Nur, 1996). Equations for the dry-rock bulk (K_{dry}) and shear (G_{dry}) moduli at a smaller porosity φ are:

$$K_{dry} = \left(\frac{\varphi / \varphi_b}{K_b + 4G_b / 3} + \frac{1 - \varphi / \varphi_b}{K_s + 4G_b / 3}\right)^{-1} - 4G_b / 3,$$
$$G_{dry} = \left(\frac{\varphi / \varphi_b}{G_b + z} + \frac{1 - \varphi / \varphi_b}{G_s + z}\right)^{-1} - z, \quad z = \frac{G_b}{6}\frac{9K_b + 8G_b}{K_b + 2G_b}. \qquad (1)$$

The effect of pore fluid can be accounted for by using Gassmann's (1951) equations.

Notice, that it is possible to arrive at the constant-cement line by first moving along the friable-sand line and then adding contact cement to the rock (dashed line in Figure 2) which is consistent with diagenesis following deposition.

ROCK PHYSICS DIAGNOSTIC APPLIED TO HEIMDAL FORMATION

The gamma-ray and P-wave velocity log curves for the two wells under examination are shown in Figure 3. In Well #1, a thick oil-saturated sand interval (gray bar in Figure 3b) is marked by extremely low and constant (about 55) gamma-ray readings and high

velocity (about 3 km/s). This sand layer is surrounded by shale packages whose gamma-ray and velocity strongly contrast those of the pay zone sand. In Well #1, unlike in Well #2, we observe a gradual variation of clay content between very clean sand and shale. Only a relatively thin (10 m) sand interval (gray bar in Figure 3d) is identified as a practically clay-free reservoir sand. The clean-sand pay zones in both wells represent the same stratigraphic unit, although located at different depths and in separate oil fields.

The velocity difference between the pay-zones in the wells under examination is emphasized in Figure 4 where the P-wave velocity is plotted versus porosity. In the same porosity range, with similar gamma-ray count, and close oil saturation, the velocity in Well #1 exceeds the velocity in Well #2 by about 500 m/s.

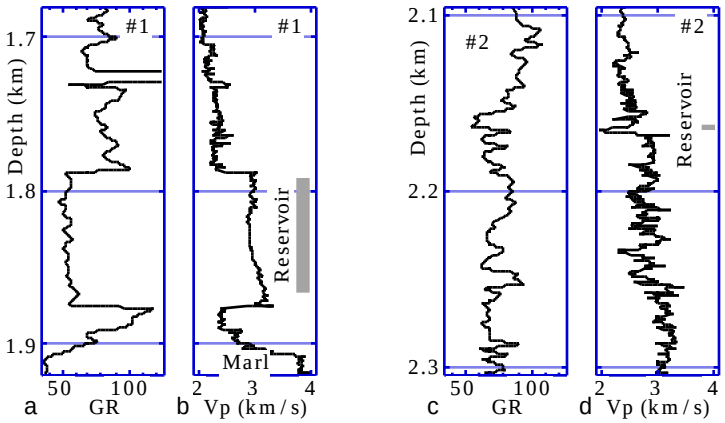

Figure 3. Gamma-ray and P-wave velocity curves for Wells #1 and #2. The clean-sand-with-oil zones are marked by gray vertical bars.

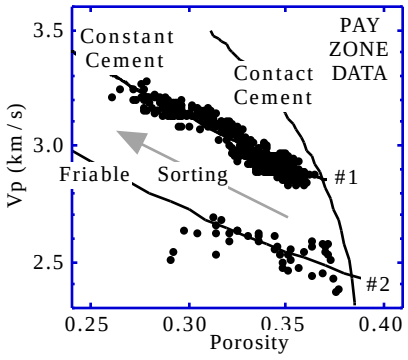

Figure 4. P-wave velocity versus porosity for the pay zones in Wells #1 and #2 with model curves superimposed. Porosity is calculated from bulk density. The arrow shows the direction of deteriorating sorting.

In order to understand the reason behind the observed velocity difference in the two wells, we superimpose the model lines on the velocity-porosity cross-plot in Figure 4.

The three curves come from the contact cement, constant cement, and friable sand models. The solid is assumed to be pure quartz; the porosity of the initial sand pack is 39%, and the initial-cement porosity φ_b is 37% (the latter corresponds to contact cement occupying about 2% of the pore space of the initial sand pack).

The rock diagnostic shown in Figure 4 implies that the pay zone sands in Well #1 have small initial contact cementation. The porosity decrease from the initial-cement porosity is likely to be due to deteriorating sorting (smaller grains falling in the pore space between larger grains with having a large effect on the velocity). The pay zones sands in Well #2 appear to lack any contact cementation with porosity reducing from the initial sand-pack porosity due to deteriorating sorting.

CONFIRMING THE DIAGNOSTIC

The thin sections of samples from both pay zones are shown in Figure 5. The porosity of both samples is about 35%. They are predominantly quartz. No contact cementation is apparent in either of the images. The Well #2 image (on the right), unlike the image from Well #1 (on the left), shows organic coating (black) around quartz grains.

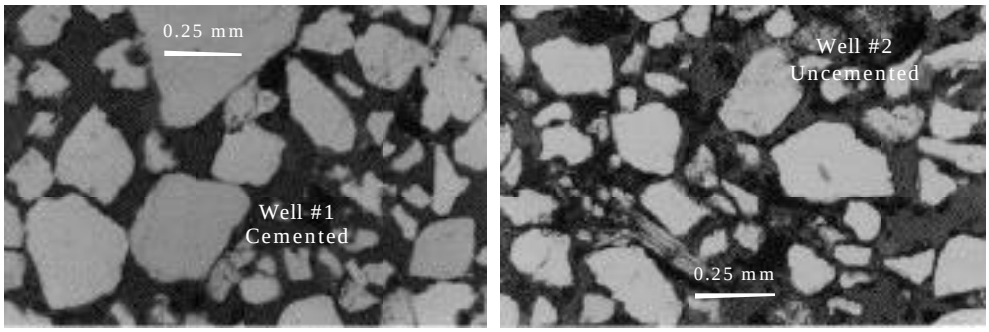

Figure 5. Thin-section images from the pay zones of Well #1 (left) and Well #2 (right).

The presence of contact cement in Well #1 reveals itself in an SEM image in Figure 6. Not detectable in the back-scatter light, it shows as a dark rim around a light grain in cathode-luminescent light. The point ERD analysis shows that both the grain and cement are pure quartz. The hexagonal crystal shapes in the upper left corner also are typical for diagenetic cementation. No cement rims or hexagonal crystal shapes have been found in the sand interval from Well #2. This thin-section analysis confirms the result of our mathematical rock diagnostic.

Consistent with this conclusion is also the fact that the cores extracted from Well #2 appeared as piles of loose sand, while those from Well #1 supported external stress. This structural integrity of the samples from Well #1 is apparently due to the binding effect of contact quartz cement.

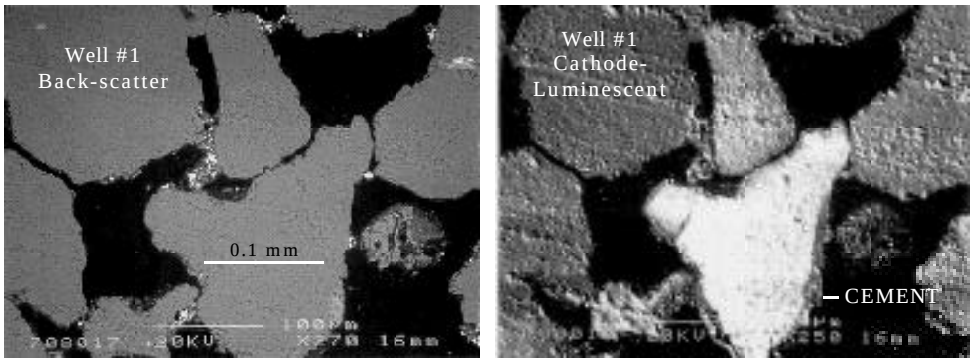

Figure 6. SEM image of a sample from the Well #1 pay zone. Left: back-scatter light; right: cathode luminescent.

Additional thin-section analysis of the Heimdal sands confirms our hypothesis that the porosity decrease in both wells is due to deteriorating sorting. The higher-porosity samples have narrow grain-size distributions and consist of equally-sized grains. On the other hand, the lower-porosity samples have large variety of grain sizes.

IMPLICATIONS FOR SEISMIC RESPONSE

To understand how the type of sand (unconsolidated versus cemented) affects the seismic response, we analyze CDP gathers at the well locations. Figure 7a shows the real CDP gather at Well #1 where the picked horizon is at the top of the Heimdal formation. Figure 7b shows a synthetic CDP gather for this well where the input (Vp, Vs and density) came from the well log measurements. This synthetic gather was produced using a 30 Hz zero-phase Ricker wavelet. The reflectivity is plotted versus offset (angle) in Figure 7e with the theoretical Zoeppritz line superimposed. The contrast in seismic properties at the shale-sand interface produces a strong positive reflector with reflectivity decreasing with increasing offset.

Contrary to Well #1, the top of the Heimdal formation in Well #2 (which is capped by similar shales) produces a weaker and negative zero-offset reflectivity that becomes increasingly negative with offset. The synthetic section shows a similar response (Figure

7d). For this well, the reflectivity is plotted versus offset (angle), together with the theoretical Zoeppritz line, in Figure 7f.

The observed significant difference in the seismic response between Well #1 and Well #2 is clearly due to the difference in sand texture (cemented versus friable).

It is important to emphasize that because the synthetic seismic response is very close to the real data in both wells, we can rely on well-log-based rock diagnostic to predict seismic response.

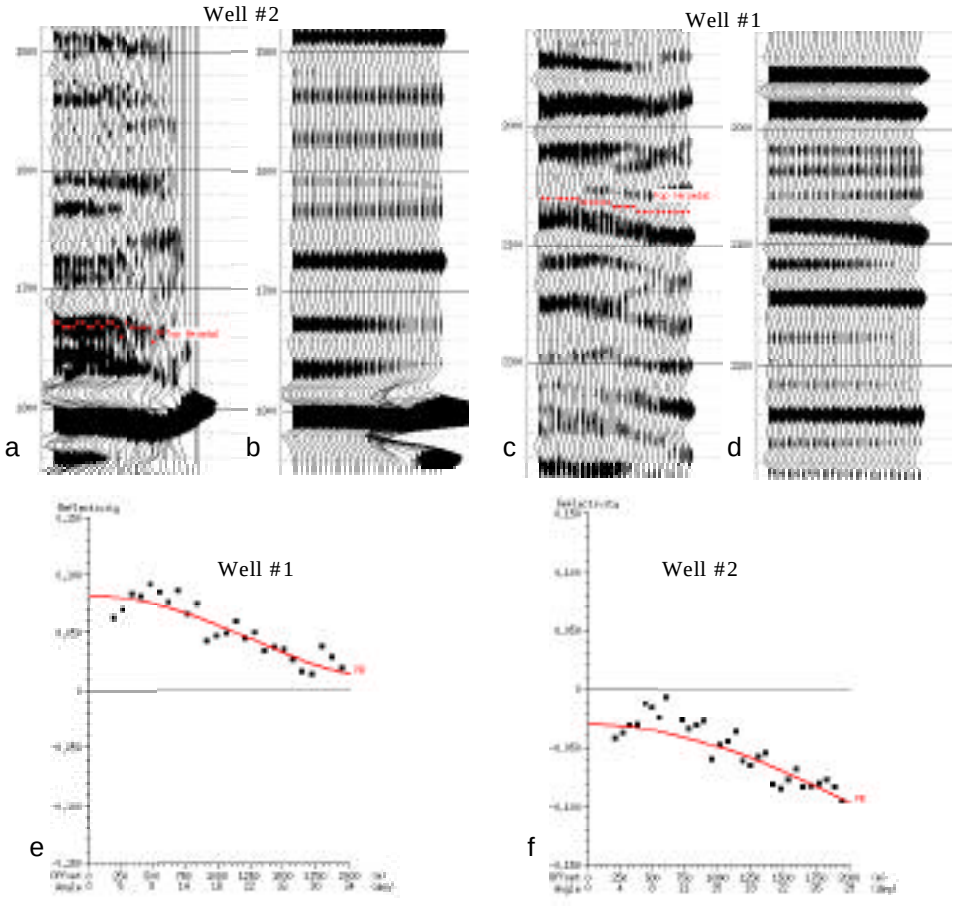

Figure 7. Top: real (a and c) and synthetic (b and d) CDP gathers. In synthetic gathers, the AVO effect was modeled only at the target zones. Bottom: real reflectivity versus offset and angle (symbols) and theoretical Zoeppritz lines.

CONCLUSIONS

- Only a few percent of contact diagenetic cement strongly affect the elastic properties of sands resulting in a drastic difference between the seismic response of slightly cemented and friable reservoirs.

- Contact cementation can be identified via rock physics diagnostic based on well log data.
- If rock diagnostic is not incorporated into seismic interpretation, the seismic-response differences may be misinterpreted as fluid or porosity changes, and result in erroneous prediction of hydrocarbons.

ACKNOWLEDGMENT

We thank Norsk Hydro for supplying the data and financial support. Additional support came from the US Department of Energy.

REFERENCES

Dvorkin, J., and Nur, A., 1996, Elasticity of High-Porosity Sandstones: Theory for Two North Sea Datasets, Geophysics, 61, 1363-1370.

Dvorkin, J., and Brevik, I., 1999, Diagnosing high-porosity sandstones: Strength and permeability from porosity and velocity, Geophysics, 64, 795-799.

Gassmann, F., 1951, Elasticity of porous media: Uber die elastizitat poroser medien, Vierteljahrsschrift der Naturforschenden Gesselschaft, 96, 1-23.

Yin, H., 1993, Acoustic velocity and attenuation of rocks: isotropy, intrinsic anisotropy, and stress induced anisotropy, Ph.D. thesis, Stanford University.